

NANO EXPRESS

Open Access



Effect of Rare-Earth Doping on Free-Volume Nanostructure of Ga-Codoped Glassy $(\text{As/Sb})_2\text{Se}_3$

Yaroslav Shpotyuk^{1,2,3}

Abstract

Subsequent stages of atomic-deficient nanostructurization finalizing rare-earth functionality under Pr^{3+} -doping in $\text{Ga}_2(\text{As}_{0.28}\text{Sb}_{0.12}\text{Se}_{0.60})_{98}$ glass are studied employing method of positron annihilation lifetime spectroscopy. Genesis of free-volume positron trapping sites, composed of atomic-accessible geometrical holes (void cores) arrested by surrounding atomic-inaccessible Se-based bond-free solid angles (void shells), are disclosed for parent As_2Se_3 , Ga-codoped $\text{Ga}_2(\text{As}_{0.40}\text{Se}_{0.60})_{98}$, as well as Ga-codoped and Sb-modified $\text{Ga}_2(\text{As}_{0.28}\text{Sb}_{0.12}\text{Se}_{0.60})_{98}$ glasses. The finalizing nanostructurization due to Pr^{3+} -doping (500 wppm) in glassy $\text{Ga}_2(\text{As}_{0.28}\text{Sb}_{0.12}\text{Se}_{0.60})_{98}$ is explained in terms of competitive contribution of changed occupancy sites available for both rare-earth ions and positrons.

Keywords: Rare-earth doping, Positron annihilation lifetime spectroscopy, Atomic-deficient nanostructurization, Sb-modification

Background

Glassy-like compounds of chalcogens (i.e., S, Se, Te) with some elements from IV-V groups of the periodic table (typically Ge, As, Sb, Bi), also known as chalcogenide glasses (ChG) [1, 2], compose a promising class of functional media for modern optoelectronics and IR optics [2–5]. Because of wide transparency window up to 20 μm accompanied by low phonon absorption, good chemical durability, and glass-forming ability, the ChG provide an excellent platform for modern fiber-optic amplifiers and mid-IR lasers [4, 5].

To be functional in many of such active photonic applications, the ChG should successfully operate as high-efficient *host* matrices for embedded *guest* activators in the form of rare-earth (RE) ions (such as Dy^{3+} , Er^{3+} , Pr^{3+}) [5]. This can be achieved by useful modification of ChG at a nanoscale level due to *nanostructurization*, the process stretching over both atomic-specific and atomic-deficient (free-volume)

structural arrangement at a nanospace. From most generalized viewpoint, such nanostructurization route includes subsequent stages of glass structure modification to meet requirements of effective *charge compensator*, *devitrification inhibitor*, and *low phonon energy RE hosting site*.

In this work, at the example of glassy arsenic selenide $\text{g-As}_2\text{Se}_3$, one of most popular ChG for waveguide optical sensing, IR lasers and telecommunication [6], we shall trace evolution of atomic-deficient glass structure during these stages (*atomic-deficient* or *free-volume nanostructurization*), employing the method of positron annihilation lifetime (PAL) spectroscopy, one of most efficient tool to study free-volume elements (FVE) in different solids (like vacancies, vacancy-type clusters, voids, pores, intrinsic cracks) at atomistic and sub-atomistic length-scales [7–10].

Methods

Nanostructurization Technologies in Chalcogenide Photonics

Nanostructurization is aimed to ensure high-efficient chemical environment in which RE ions reside homogeneously without clustering, crystallization, and phase separation.

Correspondence: yashpotyuk@gmail.com

¹Department of Sensor and Semiconductor Electronics, Ivan Franko National University of Lviv, 107, Tarnavskogo str., Lviv 79017, Ukraine

²Center for Innovation and Transfer of Natural Sciences and Engineering Knowledge, Faculty of Mathematics and Natural Sciences, University of Rzeszow, 1, Pigionia str., 35-959 Rzeszow, Poland

Full list of author information is available at the end of the article

The first stage in this row of nanostructurization technologies belongs just to glass preparation owing to conventional melt-quenching route, which is described in details elsewhere [11–13].

For this research, the ChG of stoichiometric g-As₂Se₃ (i.e., As₄₀Se₆₀) were prepared from high-purity elemental precursors, e.g., As (5 N) and Se (5 N), these ingredients being specially purified by distillation with low evaporation rate to remove impurities (such as O, C, H₂O, and SiO₂). Appropriate amounts of ingredients with total weight close to 30 g were put into silica tube of 10 mm diameter. Then, the ampoules were sealed under a vacuum, heated up to 900 °C with 2 °C/min rate and stayed at this temperature for 10 h in a rocking furnace with further quenching into water from 700 °C. To remove mechanical strains appeared during rapid quenching, the alloys were annealed for 6 h at 10 °C less than the glass transition temperature. Then, the obtained rods were cut into ~2-mm disks and polished.

The second stage in nanostructurization is to prepare the ChG with locally disturbed covalent glass-forming network possessing effective charge-compensation properties for potential RE dopants. In respect to g-As₂Se₃-based media, this can be achieved due to doping with small amount of Ga (or alternatively, In), allowing stabilization of optimal compound with maximal Ga content, but still in glassy state [14–18]. The procedure of such Ga codoping is realized via the same melt-quenching technological route as for g-As₂Se₃ using high-purity elemental Ga (7 N purity). As was shown in our preliminary research [13, 17], the Ga-codoped g-As₂Se₃ is optimized under chemical composition of g-Ga₂(As_{0.40}Se_{0.60})₉₈.

The third stage in nanostructurization is to modify the Ga-codoped ChG against possible parasitic devitrification (phase separation, crystallite nucleation, extraction, and growth), which can be activated in ChG under further RE doping. One of the best resolutions is transferring to partial As to Sb replacement in g-As-Se, allowing optimal Ga-codoped g-Ga₂(As_{0.28}Sb_{0.12}Se_{0.60})₉₈ prepared by melt-quenching route like g-As₂Se₃ or g-Ga₂(As_{0.40}Se_{0.60})₉₈ [19].

The fourth stage in nanostructurization is just finalizing RE-doping technology, i.e., the process, which is also realized under conventional melt-quenching using some precursors for RE dotation, such as Pr₂Se₃ (3 N purity). Within row of examined glassy arsenic selenides g-As-Se, this stage results in optimal g-Ga₂(As_{0.28}Sb_{0.12}Se_{0.60})₉₈ affected by RE doping with 500 wppm of Pr³⁺.

PAL Spectroscopy as Instrumentation Tool Tracing Atomic-Deficient Nanostructurization

The PAL measurements were performed using a fast-fast coincidence system of 230 ps resolution based on two Photonis XP2020/Q photomultiplier tubes coupled to BaF₂ scintillator 25.4A10/2M-Q-BaF-X-N detectors

(Scionix, Bunnik, Holland) and ORTEC® electronics (ORTEC, Oak Ridge, TN, USA). The reliable PAL spectra were detected in a normal-measurement statistics (~1 M coincidences) under stabilized temperature (22 °C) and relative humidity (35%). The channel width of 6.15 ps allows a total number of channels to be 8000. The radioactive ²²Na isotope of relatively low ~50 kBq activity prepared from aqueous solution of ²²NaCl wrapped by Kapton® foil (DuPont™, Circleville, OH, USA) of 12 μm thickness was used as positron source sandwiched between two identical tested samples.

The raw PAL spectra were processed with LT 9.0 program [20]. Under unchanged contribution from a source (with 372 ps and ~2 ns inputs), these spectra were decomposed into two normalized components with τ_{1,2} lifetimes and I_{1,2} intensities (I₁ + I₂ = 1). Under above spectrometer resolution, this allows an error-bar for such arranged measuring protocol to be not worse than ±0.005 ns in lifetimes and ±0.01 in intensities. Introducing third component in the envelope of fitting curves did not improve goodness of fitting significantly (the bound positron-electron states were not proper for studied Se-based ChG in full agreement with previous results [17, 18]).

The PAL response on atomic-deficient nanostructurization of the ChG was identified within canonical two-state positron trapping (PT) model [7–10, 21, 22], assuming that x₂-term reconstructed PAL spectrum represents only one kind of FVE. Under such circumstances, the center of mass of the reconstructed PAL spectrum coincides with average positron lifetime τ_{av} defined through normalized fractions of positron annihilation channels at defect-free bulk η_b and defect-specific η_d = τ₁·κ_d states (I₁ + I₂ = η_b + η_d = 1):

$$\tau_{av} = I_1\tau_1 + I_2\tau_2 = \eta_b\tau_b + \eta_d\tau_d. \quad (1)$$

Other physical quantities (i.e., PT-modes), in part, defect-free bulk positron lifetime τ_b and PT-rate in defects κ_d, can be calculated from x₂-term parameterized PAL spectrum as:

$$\tau_b = \tau_B = \frac{1}{\lambda_b} = \frac{\tau_1\tau_2}{I_1\tau_2 + I_2\tau_1}, \quad (2)$$

$$\kappa_d = I_2 \left(\frac{1}{\tau_1} - \frac{1}{\tau_2} \right) = \frac{I_2}{I_1} \left(\frac{1}{\tau_b} - \frac{1}{\tau_d} \right). \quad (3)$$

In addition, the (τ₂-τ_b) difference can be accepted as a size measure for extended free-volume PT sites where positrons are trapped, as well as the τ₂/τ_b ratio can be taken as direct signature of nature of these PT defects in terms of equivalent number of monovacancies [7].

Within canonical two-state PT model, the PAL response on atomic-deficient nanostructurization is defined by changes in defect-specific annihilation channel, which is determinant of PT-rate in defects κ_d [23]. Typically, these

processes are not accompanied by any changes in defect-free bulk positron lifetime τ_b , but changes in the content and sizes of PT defects (reflected in the intensity of the second component I_2 and defect-specific positron lifetime τ_2) can be essential.

The most drastic nanostructurization-induced changes concern FVE disappearance (void collapse) or, contrary, FVE appearance (void creation), the disappearing (appearing) voids being fully excluded from overall PT in ChG. Within x_2 -component PAL-spectra fitting, the PT-reduction due to FVE collapse results from decreased I_2 intensity accompanied by more slightly changed τ_2 lifetime. However, the nanostructurization can also lead to more evolutionary changes in atomic-deficient void structure, associated preferentially with nearest environment of FVE. Such evolutionary changes based on mutually opposite processes of void agglomeration (fragmentation), expansion (contraction), coarsening (refining), and charging (discharging) [23] are also finished in modified PT-rate in defects κ_d . Thus, the PT-reduction owing to *agglomeration* of relatively large voids, which get favorable environment to grow in size owing to their merge [23, 24], is accompanied by decrease in I_2 intensity and slight increase in τ_2 lifetime. At the same time, the PT-enhancement (i.e., increase in the PT-rate κ_d) determines *fragmentation* of relatively large free-volume voids, which tend to be tiny owing to grinding (decaying on separate parts), this process being accompanied by increased I_2 intensity and decreased defect-related τ_2 lifetime.

Results and Discussion

Let us trace evolution of atomic-deficient (free-volume) nanostructurization over four subsequent stages (parent glass—Ga-codoping—Sb-modification—RE doping) using the PAL spectroscopy data for typical samples of arsenic selenide ChG.

The measured raw PAL spectra are reconstructed from x_2 -term fitting procedure, these spectra for parent $g\text{-As}_2\text{Se}_3$, Ga-codoped $g\text{-Ga}_2(\text{As}_{0.40}\text{Se}_{0.60})_{98}$, Ga-codoped and Sb-modified $g\text{-Ga}_2(\text{As}_{0.28}\text{Sb}_{0.12}\text{Se}_{0.60})_{98}$, Pr^{3+} -doped (500 wppm) $g\text{-Ga}_2(\text{As}_{0.28}\text{Sb}_{0.12}\text{Se}_{0.60})_{98}$ being depicted on Fig. 1. The limited values of scatter of variance tightly grouped along 0-axis testify that PAL probing is adequately described within this fitting procedure. Therefore, decaying behavior of the PAL spectra on Fig. 1 can be reflected by sum of two negative exponentials with different time constants inversed to positron lifetimes. The best-fit positron trapping modes for the examined ChG calculated within two-state PT model [7–10, 21, 22] are given in Table 1.

Free-Volume Nanostructurization in Parent $g\text{-As}_2\text{Se}_3$

The parent $g\text{-As}_2\text{Se}_3$ possesses defect-specific lifetime $\tau_2 = 0.360$ ns (Table 1) proper to this ChG as it follows from numerous previous research [25–28]. The positron trapping in $g\text{-As}_2\text{Se}_3$ is defined by PT-rate $\kappa_d = 0.92$ ns⁻¹ occurring under fraction of trapped positrons $\eta_d = 0.19$. In respect to Jensen et al.'s DFT-calculations for orthorhombic As_2Se_3 crystal [27], this lifetime gives an

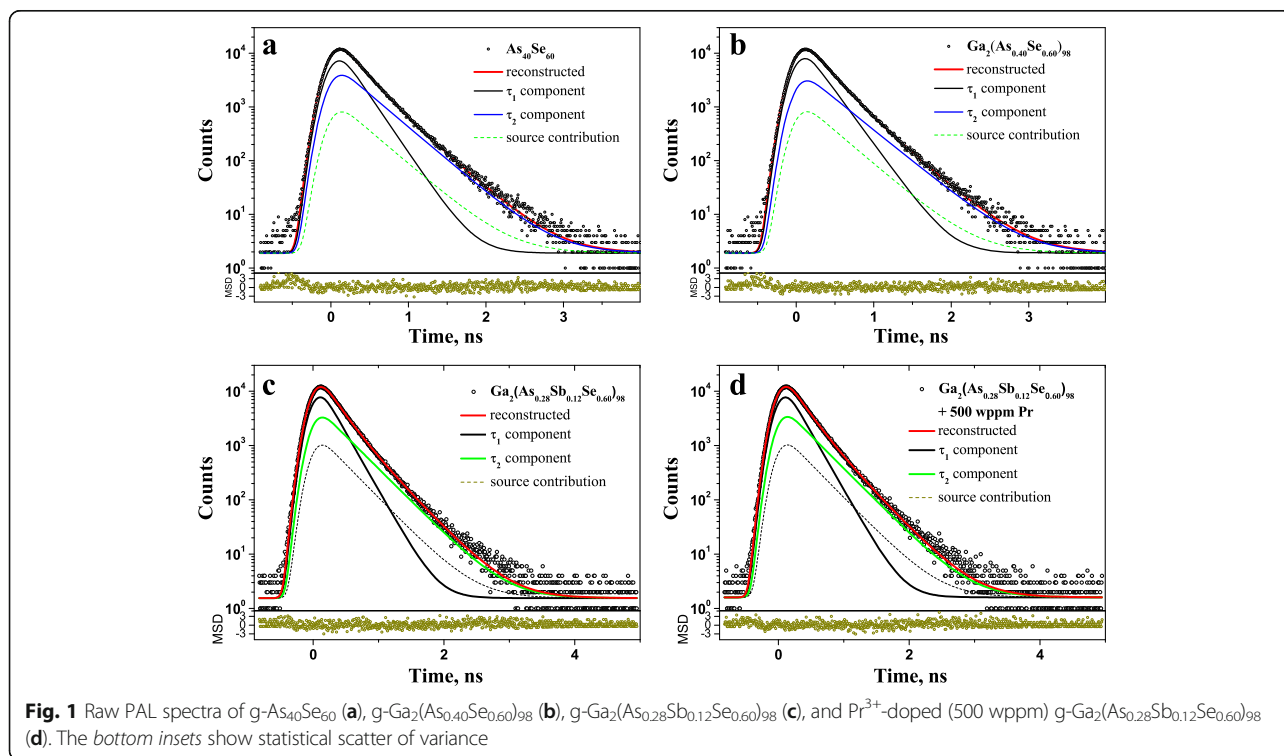


Table 1 Fitting parameters and PT-modes describing two-component reconstructed PAL spectra in $g\text{-Ga}_x[(\text{As}/\text{Sb})_{0.40}\text{Se}_{0.60}]_{100-x}$

ChG sample	Fitting parameters			Positron trapping modes					
	τ_1	τ_2	I_2	τ_{av}	τ_b	κ_d	$\tau_2 - \tau_b$	τ_2/τ_b	η_d
	ns	ns	a.u.	ns	ns	ns^{-1}	Ns	–	–
$g\text{-As}_{40}\text{Se}_{60}$	0.210	0.360	0.462	0.279	0.260	0.92	0.10	1.39	0.19
$g\text{-Ga}_2(\text{As}_{0.40}\text{Se}_{0.60})_{98}$	0.223	0.382	0.401	0.287	0.267	0.75	0.11	1.43	0.17
$g\text{-Ga}_2(\text{As}_{0.28}\text{Sb}_{0.12}\text{Se}_{0.60})_{98}$	0.210	0.363	0.422	0.274	0.255	0.85	0.11	1.42	0.18
Pr^{3+} -doped (500 wppm)	0.218	0.374	0.376	0.276	0.258	0.72	0.12	1.45	0.16
$g\text{-Ga}_2(\text{As}_{0.28}\text{Sb}_{0.12}\text{Se}_{0.60})_{98}$									

estimate for volume of PT defects near $\sim 90 \text{ \AA}^3$. This open volume corresponds to 0.10 ns in ($\tau_2 - \tau_b$) difference and 1.39 in τ_2/τ_b ratio, which can be accepted as a signature of extended triple-quadruple vacancies [7, 27]. It is difficult to define exactly which part of this free volume is atomic-accessible in glassy network in view of complicated inner structural configuration composed of interconnected atom-shared $\text{AsSe}_{3/2}$ pyramids in $g\text{-As}_2\text{Se}_3$. In ref. [17], possible configuration of such PT free-volume voids were depicted at the map of electron-density distribution for isostructural mineral orpiment As_2S_3 .

Structural genesis of expected PT sites in parent $g\text{-As}_2\text{Se}_3$ is conditionally illustrated on Fig. 2a assuming close to ellipsoidal shape for free-volume voids. The most efficient preferential PT sites are defined by extended free-volume spaces near Se atoms neighboring with $\text{AsSe}_{3/2}$ polyhedrons [26, 27]. Because of strong directionality of covalent chemical bonding in ChG, Se atoms form lower electron-density spaces known as *bond-free solid angles* (BFSA) in terms of Kastner [29]. These *atomic-inaccessible BFSA* contribute to neighboring geometrical free volumes, ensuring effective negative electrical charge due to proximity with electronegative Se atoms linked with more electropositive As. So, the BFSA originated from Se atoms form *outer shell* for *inner geometrical hole* of free-volume void, which can be identified in view of its preferential electric state as counterparts of cation-type vacancy in crystals [7].

Therefore, the most efficient PT sites in $g\text{-As}_2\text{Se}_3$ can be imaged as free-volume voids formed within network of interlinked corner-shared $\text{AsSe}_{3/2}$ pyramids, composed of atomic-accessible geometrical hole (*void core*) arrested by surrounding atomic-inaccessible Se-based BFSA (*void shell*), as it is illustrated in Fig. 2.

Free-Volume Nanostructurization Under Ga-Codoping

Effect of Ga-codoping in parent $g\text{-As}_2\text{Se}_3$, i.e., transition from $g\text{-As}_2\text{Se}_3$ to $g\text{-Ga}_2(\text{As}_{0.40}\text{Se}_{0.60})_{98}$, is revealed through gradual dropping in I_2 intensity accompanied by increase in defect-specific τ_2 lifetime to 0.382 ns (Table 1). At the basis of Jensen et al.'s [27] formalism, the latter can be ascribed to free volumes reaching as high as $\sim 110 \text{ \AA}^3$. This jump in defect-specific τ_2 lifetime is ascribed to increased average atomic coordination $Z = 2.412$ of $g\text{-Ga}_2(\text{As}_{0.40}\text{Se}_{0.60})_{98}$ due to Ga addition. Under such condition, the appeared $\text{Se}_{2/2}\text{-As-As-As-Se}_{2/2}$ bridges counterbalance Ga additions in $g\text{-As-As-Se}$, causing increased number of overlapped BFSA around end-terminated Se atoms contributing to PT sites [17, 28]. Thus, the Ga-codoping in $g\text{-As}_2\text{Se}_3$ results in *agglomeration* of existing PT sites (increase in their volume, but decrease in their content), thus leading to gradual decrease in PT-rate in defects κ_d and, correspondingly, the fraction of trapped positrons η_d (see Table 1).

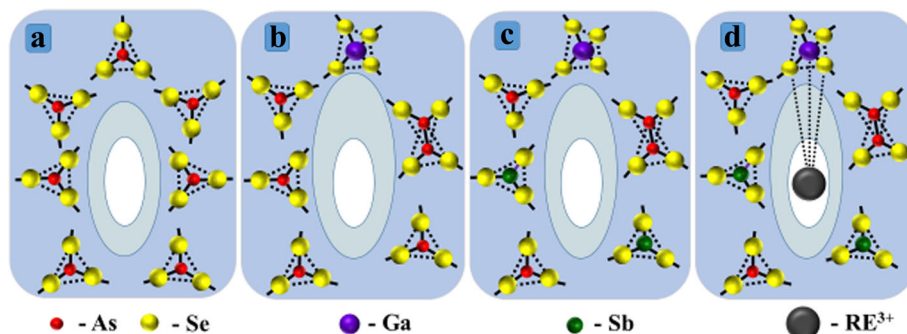


Fig. 2 Genesis of free-volume PT-site in $g\text{-As-Se}$ under subsequent nanostructurization stages evolving parent $g\text{-As}_{40}\text{Se}_{60}$ (a), Ga-codoped $g\text{-Ga}_2(\text{As}_{0.40}\text{Se}_{0.60})_{98}$ (b), Ga-codoped and Sb-modified $g\text{-Ga}_2(\text{As}_{0.28}\text{Sb}_{0.12}\text{Se}_{0.60})_{98}$ (c), and Pr^{3+} -doped (500 wppm) $g\text{-Ga}_2(\text{As}_{0.28}\text{Sb}_{0.12}\text{Se}_{0.60})_{98}$ (d). The inner atomic-accessible free-volume core is marked by *white color*, the outer atomic-inaccessible free-volume shell is *blue-light-shadowed*, while surrounding glassy network composed by different glass-forming polyhedrons is *blue-dark-shadowed* (see text for more details)

It is worth to note that PAL response on Ga-induced nanostructurization is fully determined by chemical composition of parent ChG. Thus, for example, in case of smaller $Z = 2.30$ character for TAS-235 glass (i.e., g-As₃₀Se₅₀Te₂₀) [18], Ga-codoping does not change defect-specific τ_2 lifetime, despite more pronounced decrease in I_2 intensity. This result is fully concomitant with small deviations observed in τ_2 lifetimes for Se-rich ChG compositions in As-Se system [26, 28].

In general, such modification (when only atomic-deficient free-volume structure is changed) is unable to accommodate RE ions obeying electrically active state (RE³⁺), avoiding non-radiative decay [5, 14, 17, 18]. The FVE-accommodated RE dopants have to adopt an excess of positive electrical charge to ensure electrical compensation throughout a glassy matrix. Successful resolution is based on possibility of Ga-codopants to reveal a metallic behavior being inserted in chalcogenide environment. In interaction with chalcogens, the Ga atoms create some polyhedrons (such as GaSe_{4/2} tetrahedra shown in the upper part on Fig. 2b), which are, from one side, topologically consistent with main network-forming polyhedrons to attain unique glassy arrangement having a large number of voids, but, from other side, these codopants can stabilize charge misbalance owing to local chalcogen (Se) over-coordination around Ga [14, 16, 30]. Under transition to g-Ga₂(As_{0.40}Se_{0.60})₉₈, the GaSe_{4/2} tetrahedrons with favorable Ga-Se chemical bonds appear in a network of corner-shared AsSe_{3/2} pyramids forming overall glassy matrix. Excess of anion-type atoms occupying Se²⁻ states around GaSe_{4/2} tetrahedrons causes the cloud of preferentially negative electrical charge for neighboring free-volume void (as it is shown by enlarged outer shell in the constitution of PT site on Fig. 2b). In such a way, the more negatively charged voids of increased overall free volume in Ga-modified g-Ga₂(As_{0.40}Se_{0.60})₉₈ serve as eventual precursors for *charge-compensating incorporation* of electrically active Pr³⁺ ions.

Free-Volume Nanostructurization Under Sb-Modification

One of the parasitic drawbacks of Ga-codoping nanostructurization concerns in increased crystallization ability of Ga-contained ChG under further RE doping, since both Ga and RE chalcogenides possess isostructural crystalline polymorphs [5, 13]. In case of As-based ChG, this obstacle can be suppressed under partial As-to-Sb replacement [19]. This was a reason to turn towards nanostructurization in g-As-Se under Sb-modification.

In respect to atomic-deficient structure evidenced from PAL spectroscopy, this Sb-substituted g-Ga₂(As_{0.28}Sb_{0.12}Se_{0.60})₉₈ demonstrates partial recovery to parent pure g-As₂Se₃. Indeed, in this ChG, the defect-specific lifetime τ_2 is depressed down to 0.363 ns and

second component intensity I_2 gets elevated to 0.422, thus resulting in steadily increasing PT-rate in defects with $\kappa_d = 0.85 \text{ ns}^{-1}$ (Table 1). This Sb-modification is not accompanied by change in PT-site type, since neither ($\tau_2 - \tau_b$) difference, nor τ_2/τ_b ratio remains rather unchanged within measuring error-bar.

Such effects are supposed to be defined by increase in an atomic packing of glassy network due to heavier (and more metallic) Sb atoms appeared instead of As ones (causing respective increase in ChG density from 4.64 to 4.90 g/cm³ [19]). On Fig. 2c, these Sb-based structural entities are presented as SbSe_{3/2} pyramidal units appeared in the nearest atomic surrounding of free-volume void. So PT sites in Sb-modified g-Ga₂(As_{0.28}Sb_{0.12}Se_{0.60})₉₈ are like those in g-Ga₂(As_{0.40}Se_{0.60})₉₈, but with slightly reduced outer free-volume shell mainly due to shielding effect from more metallic Sb-environment (Fig. 2c).

Free-Volume Nanostructurization Under RE Doping

Thus, in respect to these subsequent nanostructurization stages, the effect of RE doping can be treated in terms of *competitive contribution of changed occupancy sites* in the modified structure of g-Ga₂(As_{0.28}Sb_{0.12}Se_{0.60})₉₈ available for both RE ions and positrons. Indeed, from the point of affinity to negative electrical charge attached to neighboring free-volume space, the same type of voids, which accommodate RE³⁺ ions, as shown in Fig. 2d, can be attractive sites for annihilating positrons [6–10]. Under RE doping, the positively charged Pr³⁺ ions are stabilized in a glassy network due to strong Pr³⁺-Se-Ga covalent bridges (marked by dotted lines in Fig. 2d) [14, 31, 32], thus eliminating corresponding negatively charged void as potential positron traps. This void-collapse process results in PT-reduction, mainly due to essential decrease in second component intensity I_2 and rather slight increase in defect-specific lifetime τ_2 (see Table 1), meaning that void volume is not essentially altered under RE doping.

Concentration of these PT free-volume defects in RE-doped ChG can be estimated accepting their analogy with negative cation-type vacancies in semiconductors giving trapping coefficients of approximately 10¹⁵ atom·s⁻¹ [7]. With known atomic densities and experimental PT-rate value for different ChG (Table 1), this estimation gives the defect concentration close to $\sim 5 \cdot 10^{16} \text{ cm}^{-3}$. It means that under a condition of full identity to void occupation for both annihilating positrons and embedded RE ions, the effect of RE doping can be detected at very low concentrations (reaching only tens of wppm). That is why the PAL spectroscopy can be successfully applied to study RE doping in glassy substances, where conventional atomic-sensitive probes such as X-ray, electron, or neutron diffraction are ineffective because of under-

margin content of embedded RE ions, which is typically beyond reliably detectable limits of these methods.

Conclusions

Atomic-deficient evolution of glassy arsenic selenides is traced in subsequent nanostructurization stages ensuring their RE-doping functionality, the positron annihilation lifetime spectroscopy being employed to parameterize free-volume positron trapping sites within known two-state trapping model. The most efficient positron traps in parent As_2Se_3 glass are imagined as voids with character free volumes of $\sim 90 \text{ \AA}^3$ formed in network of corner-shared $\text{AsSe}_{3/2}$ pyramids, composed of atomic-accessible geometrical holes (void cores) arrested by surrounding atomic-inaccessible Se-based bond-free solid angles (void shell). Under Ga-codoping in $\text{Ga}_2(\text{As}_{0.40}\text{Se}_{0.60})_{98}$ glass, these voids grow in size, being essentially modified by their environment to become preferentially negative, thus serving as precursors for charge-compensating incorporation of electrically active rare-earth ions. Vitreous state stabilizing modification with Sb additives reduces outer free-volume shell of positron trapping sites mainly due to shielding effect from more metallic environment. The finalizing nanostructurization under Pr^{3+} -doping (500 wppm) in $\text{Ga}_2(\text{As}_{0.28}\text{Sb}_{0.12}\text{Se}_{0.60})_{98}$ glass is explained in terms of competitive contribution of changed occupancy sites available for both rare-earth ions and positrons.

Abbreviations

BFSA: Bond-free solid angles; ChG: Chalcogenide glasses; FVE: Free-volume elements; PAL: Positron annihilation lifetime; PT: Positron trapping; RE: Rare-earth

Acknowledgements

With a great pleasure I thank B. Bureau, C. Boussard-Pledel, and V. Nazabal (Glass and Ceramics Laboratory of University of Rennes 1) for their helpful assistance during glass preparation and input characterization. The valuable consulting on PALS experiments provided by Dr. Adam Ingram (Opole University of Technology) is also highly acknowledged.

Competing Interests

The author declares that he has no competing interests.

Author details

¹Department of Sensor and Semiconductor Electronics, Ivan Franko National University of Lviv, 107, Tarnavskogo str., Lviv 79017, Ukraine. ²Center for Innovation and Transfer of Natural Sciences and Engineering Knowledge, Faculty of Mathematics and Natural Sciences, University of Rzeszow, 1, Pigionia str., 35-959 Rzeszow, Poland. ³Laboratoire Verres et Céramiques, UMR-CNRS 6226, Université de Rennes 1, 35042 Rennes Cedex, France.

Received: 13 December 2016 Accepted: 27 February 2017

Published online: 14 March 2017

References

- Feltz A (1986) Amorphous and vitreous inorganic solids. Mir, Moscow
- Adam JL, Zhang X (eds) (2014) Chalcogenide glasses: preparation, properties and applications. Woodhead publishing, Oxford-Cambridge-New Delhi
- Cui S, Chahal R, Shpotyuk Y, Boussard C et al (2014) Selenide and telluride glasses for mid-infrared biosensing. *Proc SPIE* 8938:893805
- Lucas P, Bureau B (2017) Selenide glass fibers for biochemical infrared sensing. In: Ahluwalia GK (ed) Applications of Chalcogenides: S, Se, and Te. Springer, Cham, pp 285–322
- Seddon AB, Tang Z, Furniss D, Sujecki S, Benson TM (2010) Progress in rare-earth-doped mid-infrared fiber lasers. *Opt Express* 18:26704–26719
- Troles J, Coulombier Q, Canat G et al (2010) Low loss microstructured chalcogenide fibers for large nonlinear effects at 1995 nm. *Opt Express* 18:26647–26654
- Krause-Rehberg R, Leipner H (1999) Positron annihilation in semiconductors: defect studies. Springer, Heidelberg
- Jean YC, Mallon PE, Schrader DM (2003) Principles and application of positron and positronium chemistry. World Sci. Publ. Co. Pte. Ltd., New Jersey-London-Singapore-Hong Kong
- Tuomisto F, Makkonen I (2013) Defect identification in semiconductors with positron annihilation: experiment and theory. *Rev Mod Phys* 85:1583–1631
- Shpotyuk O, Filipecki J (2003) Free volume in vitreous chalcogenide semiconductors: possibilities of positron annihilation lifetime study. *WSP, Czestochowa*
- Shpotyuk Y, Bureau B, Boussard-Pledel C, Nazabal V, Golovchak R, Demchenko P, Polovynko I (2014) Effect of Ga incorporation in the $\text{As}_{30}\text{Se}_{50}\text{Te}_{20}$ glass. *J Non-Cryst Solids* 398–399:19–25
- Shpotyuk O, Ingram A, Bureau B, Shpotyuk Y, Boussard-Pledel C, Nazabal V, Szatanik R (2014) Positron annihilation probing of crystallization effects in TAS-235 glass affected by Ga additions. *J Phys Chem Solids* 75:1049–1053
- Shpotyuk Y, Boussard-Pledel C, Nazabal V, Chahal R, Ari J, Pavlyk B, Cebulski J, Doualan JL, Bureau B (2015) Ga-modified As_2Se_3 -Te glasses for active applications in IR photonics. *Opt Mater* 46:228–232
- Aitken BG, Ponader CW, Quimby RS (2002) Clustering of rare earths in GeAs sulfide glass. *CR Chimie* 5:865–872
- Churbanov MF, Scribachev IV, Shiryaev VS, Plotnichenko VG, Smetanin SV, Kryukova EB, Pyrkov YN, Galagan BI (2013) Chalcogenide glasses doped with Tb, Dy and Pr ions. *J Non-Cryst Solids* 326–327:301–305
- Golovchak R, Shpotyuk Y, Nazabal V, Boussard-Pledel C, Bureau B, Cebulski J, Jain H (2015) Study of Ga incorporation in glassy arsenic selenides by high-resolution XPS and EXAFS. *J Chem Phys* 142:184501
- Shpotyuk Y, Ingram A, Shpotyuk O, Dziedzic A, Boussard-Pledel C, Bureau B (2016) Free-volume nanostructurization in Ga-modified As_2Se_3 glass. *Nanoscale Res Lett* 11:20
- Shpotyuk Y, Ingram A, Shpotyuk O, Boussard-Pledel C, Nazabal V, Bureau B (2016) Effect of rare-earth doping on the free-volume structure of Ga-modified $\text{Te}_{20}\text{As}_{30}\text{Se}_{50}$ glass. *RSC Adv* 6:22797–22802
- Shpotyuk Y, Boussard-Pledel C, Nazabal V, Bureau B (2017) The influence of Sb on glass forming ability of Ga-containing As_2Se_3 glasses. *J Am Ceram Soc.* doi:10.1111/jace.14662
- Kansy J (1996) Microcomputer program for analysis of positron annihilation lifetime spectra. *Nucl Instrum Methods Phys Res, Sect A* 374:235–244
- Seeger A (1974) The study of defects in crystals by positron annihilation. *Appl Phys* 4:183–199
- Keeble DJ, Brossmann U, Puff W, Würschum R (2012) Positron annihilation studies of materials. In: Kaufmann EN (ed) Characterization of materials. John Wiley & Sons, Inc., pp 1899–1925
- Shpotyuk M, Ingram A, Shpotyuk O (2015) Characterization of radiation-induced effects in amorphous arsenic sulfides by positron annihilation. *J Mater Res* 30:1422–1429
- Ghosh S, Nambissan PMG, Bhattacharya R (2004) Positron annihilation and Mössbauer spectroscopic studies of In^{3+} substitution effects in bulk and nanocrystalline $\text{MgMn}_{0.1}\text{Fe}_{1.9-x}\text{In}_x\text{O}_4$. *Phys Lett A* 325:301–308
- Alekseeva OK, Mihailov VI, Chernov AP, Shantarovich VP (1977) Point structural defects studied in chalcogenide semiconductors by positron annihilation. *Sov Fiz Tverd Tela* 19:3452–3454
- Alekseeva OK, Mihajlov VI, Shantarovich VP (1978) Positron annihilation in point defects of the glassy As-Se system. *Phys Stat Solidi A* 48:K169–K173
- Jensen KO, Salmon PS, Penfold IT, Coleman PG (1994) Microvoids in chalcogenide glasses studied by positron annihilation. *J Non-Cryst Solids* 170:57–64
- Ingram A, Golovchak R, Kostrzewa M, Wacke S, Shpotyuk M, Shpotyuk O (2012) Compositional dependences of average positron lifetime in binary As-S/Se glasses. *Phys B* 407:652–655
- Kastner M (1973) Compositional trends in the optical properties of amorphous lone-pair semiconductors. *Phys Rev B* 7:5237–5252

30. Golovchak R, Shpotyuk Y, Thomas CM, Nazabal V, Boussard-Pledel C, Bureau B, Jain H (2015) Peculiarities of Ga and Te incorporation in glassy arsenic selenides. *J Non-Cryst Solids* 429:104–111
31. Lee TH, Simdyankin SI, Su L, Elliott SR (2009) Evidence of formation of tightly bound rare-earth clusters in chalcogenide glasses and their evolution with glass composition. *Phys Rev B* 79:180202
32. Lee TH, Simdyankin SI, Hegedus J, Heo J, Elliott SR (2010) Spatial distribution of rare-earth ions and GaS₄ tetrahedra in chalcogenide glasses studied via laser spectroscopy and ab initio molecular dynamics simulation. *Phys Rev B* 81:104204

Submit your manuscript to a SpringerOpen[®] journal and benefit from:

- ▶ Convenient online submission
- ▶ Rigorous peer review
- ▶ Immediate publication on acceptance
- ▶ Open access: articles freely available online
- ▶ High visibility within the field
- ▶ Retaining the copyright to your article

Submit your next manuscript at ▶ springeropen.com
